Temperature-induced Chemical Changes in Soundless Chemical Demolition Agents

Atteyeh S. Natanzi[a], Debra F. Laefer[b], Glikeria Kakali[c], S.M. Iman Zolanvari[d]

[a]Post-doctoral Research Fellow, School of Civil Engineering, University College Dublin, Newstead Building, Belfield, Dublin 4, Ireland; Atteyeh.natanzi@ucdconnect.ie

[b]Professor, Center for Urban Science and Progress and Department of Civil and Urban Engineering, Tandon School of Engineering, New York University, 370 Jay St. 12th Fl, Brooklyn, NY 11201; School of Civil Engineering, University College Dublin, Newstead Building, Belfield, Dublin 4, Ireland

Corresponding Author: Debra.Laefer@nyu.edu

[c]Professor, School of Chemical Engineering, National Technical University Athens (NTUA), Iroon Polytechneiou 9, Zografou 157 80, Athens, Greece; Kakali@central.ntua.gr

[d]Postdoctoral Researcher, School of Computer Science and Statistics, Trinity College Dublin, College Green, Dublin 2, Ireland; Iman.zolanvari@ucdconnect.ie

Abstract: This paper explores the relationship between ambient temperature, calcium oxide (CaO) hydration, and calcium carbonate ($CaCO_3$) generation in cold and moderate ambient temperatures (2°C-19°C). A total of 22 samples from 2 commercial Soundless Chemical Demolition Agents (SCDAs) were tested in 36 mm diameter, 170 mm long steel pipes. The raw powder and materials resulting from hydration were subjected to X-ray Diffraction analysis, Derivative Thermogravimetric Analysis, and Thermogravimetry analysis. Raw and hydrated specimens proved chemically distinctive. Experimental results showed: (1) the unconfined portions of hydrated specimens contained more $CaCO_3$ due to carbonation of $Ca(OH)_2$, where confined portions had higher $Ca(OH)_2$ concentrations; (2) all materials tested at 19°C ambient temperatures had $Ca(OH)_2$ concentrations nearly 10% greater than those tested at 2°C; and (3) the higher $Ca(OH)_2$ concentrations formed at 19°C generated 350% greater expansive pressure than that which formed at 2°C.

Keywords: Soundless Chemical Demolition Agents, Hydration, Ettringite, Calcium Hydroxide, Temperature, X-Ray Diffraction, Thermogravimetry analysis

Introduction

Demolition in environmentally sensitive areas is challenging due to noise and vibration limits and prohibitions against usage of explosive agents. Traditional demolition methods such as jackhammers, controlled blasting, and diamond wire cutting produce large levels of noise, vibration, and/or dust. In such cases, Soundless Chemical Demolition Agents (SCDAs) (also known as Non-Explosive Expansion Materials) offer a silent, vibrationless alternative. This paper explores the relationship between ambient temperature, calcium oxide (CaO) hydration, and calcium carbonate ($CaCO_3$) generation in cold and moderate ambient temperatures for two prominent SCDA brands. Understanding the distribution and concentration of calcium oxide (CaO) hydration within a mass of SCDA could significantly improve the understanding of expansive pressure generation and, thus, ensure more predictable SCDA application and aid in the geometric optimization of installation cavities, which are currently only done as vertical cylinders (e.g. Natanzi and Laefer, 2014).

Background

SCDAs were first identified by Cadlot and Micheaelis in the 1890s when ettringite in cement was investigated (Mather 1970). Nearly 100 years later, the first commercial SCDA was developed in Japan in 1979 (Hayashi et al. 1993). In 1982, a slow acting SCDA was reported to crack concrete in 4-5 days. Despite SCDA's advantages, such long demolition

47 times were considered problematic. Thus, three years later, a faster acting agent was
48 introduced to demolish concrete within only three hours (Hayashi et al. 1993). Most of
49 today's commercial products promise initial cracking within a few hours, but actual
50 performance is highly variable and extremely temperature dependent, as a direct function
51 of the material's chemical composition.
52
53 An SCDA is typified by being a manufactured material that is naturally hygroscopic, non-
54 combustible, and non-explosive (Étkin and Azarkovich 2006). SCDAs are generally grayish,
55 powdery materials, like Portland cement, that consist of calcium oxide (CaO) (often over
56 90%) and different amounts of ferric oxide (Fe_2O_3), magnesium oxide (MgO), aluminum
57 oxide (Al_2O_3), silicon (SiO_2), Portland cement, clinker materials, and calcium fluoride
58 (CaF_2). While calcium oxide (CaO) is the main SCDA ingredient, other materials have been
59 added to change, enhance, postpone, or control the hydration procedure (Hinze and Brown
60 1994). The presence of binders is known to decrease the amount of calcium oxide (CaO) in
61 the mixture and, in turn, reduce the thermal effects and subsequent stress development
62 (Étkin and Azarkovich 2006).
63
64 After mixing with water, the main chemical reaction is hydration of the calcium oxide
65 (CaO), which generates heat and, subsequently, expansive pressure. This is as represented
66 in Eqn 1 as proposed by Goto et al. (1988):
67 $$CaO + H_2O \rightarrow Ca(OH)_2 + 15.2 \uparrow (kCal/mol) \quad (1)$$
68 As calcium oxide hydration develops, other cement components such as alite (tricalcium
69 silicate) may also hydrate (Soeda and Harada 1994). Hydration of the calcium oxide and

formation of ettringite and calcium hydroxide ($Ca(OH)_2$) generate tensile stress and volumetric expansion. Ettringite formation is based on the reaction of calcium aluminate with calcium hydroxide, calcium sulphate, and water as shown in Eqn 2 (Cohen and Richards 1982).

$$3CaO.3Al_2O_3.CaSO_4 + 6Ca(OH)_2 + 90H_2O \rightarrow 3(3CaO.Al_2O_3.3CaSO_4.32H_2O) \quad (2)$$

There are multiple theories and models explaining ettringite formation and expansion, but they can be divided into two main groups: (1) crystal growth theory and (2) swelling theory. Crystal growth theory hypothesizes that expansion is caused by increasing quantities of ettringite crystals, which form on the surfaces of the SCDA particles or in the resulting solution. This crystal growth causes a crystallisation pressure and then an expansive pressure gain. In contrast, swelling theory hypothesizes that expansion is caused by water-adsorption and the swelling characteristics of the ettringite gel, which form by means of a through-solution mechanism due to the reaction between the expansive particles and the surrounding solution. The presence of calcium hydroxide ($Ca(OH)_2$) in solution results in the formation of colloidal-sized ettringite particles, and the absence of calcium hydroxide ($Ca(OH)_2$) results in the creation of larger ettringite particles (Cohen 1983). In recent research by De Silva et al. (De Silva et al. 2017), SCDA hydration and crystal growth generation in Bristar were investigated at different hydration times (1 h, 6 h, 12 h, 16 h, 20 h and 24 h). The scanning electron microscopy (SEM) analysis showed three different crystal formations in the hydrated SCDA: the clear form of Portlandite, the prismatic needle shape of Ettringite, and the amorphous Calcium Silicate Hydrate (CSH), which reduced with time. Based on these results, the authors claimed that the formation of calcium hydroxide ($Ca(OH)_2$) and ettringite contribute to expansive pressure development,

but that the process is dominated by calcium hydroxide ($Ca(OH)_2$) formation. For a further discussion of these processes, the readers are referred to the following references (Aqel and Panesar 2017; Mehta 1973; Taylor et al. 2001).

The chemical changes during the hydration of SCDA can influence the expansive pressure development directly. To investigate the mechanism of hydration and expansive pressure development, a detailed mineralogical analysis was conducted using X-ray Diffraction analysis (XRD) and Thermogravimetry analysis (TG) analysis.

Understanding the hydration process is important as it influences pressure development. Specifically, experiments by Soeda et al. (1994) in steel pipes with two types of SCDAs (one for warm and one for cold temperatures) demonstrated that higher hydration levels increased expansive pressure development. After hydration occurs, stresses form inside the pre-drilled hole. When those exceed the strength of the surrounding material, cracks will initiate and propagate (Étkin and Azarkovich 2006). This process requires a period of time from a few hours to several days depending upon the SCDA, the surrounding temperature, the strength of the surrounding material, the borehole diameter and depth, and the slurry composition (Laefer et al. 2010). SCDA formulation and mixing water temperature can significantly affect the ettringite formation rate and, in turn, the speed and magnitude of expansive pressure development (Polivka 1973).

While SCDAs are designed to be applied over a wide range of ambient temperatures (0°C to 40°C), outdoor temperature changes in a single day can impact significantly the onset and

level of pressure development, especially in cool to moderate temperatures. In such temperatures, tests on large-scale unreinforced concrete blocks, Huynh and Laefer (2009) showed that the Time to First Crack (TFC) and the Minimum Demolition Time (MDT) [moment at which there is sufficient cumulative cracking width for non-percussive, mechanical material removal] increased when the temperature was only a few degrees lower. Dowding and Labuz (1982) showed, in thick-walled, steel cylinder tests, that decreasing the ambient temperature from 25˚C to 15˚C directly decreased the expansive pressure by 38% after 24 hours and 10% after 48 hours. Similarly, The Onoda Cement Company (1980) reported a 30% decrease in expansive pressure at 24 hours and a 10% decrease at 48 hours in thin-walled steel cylinders when the ambient temperature was reduced from 25°C to 15°C.

In higher temperature tests with SCDAs in steel tubes, Hinze and Brown (1994) observed disproportionate pressure changes with temperature. After 24 hours, the pressure at 45°C was double that recorded at 30°C and four-fold of that at 20°C. SCDA testing in 1 m^3 concrete blocks with small aggregate showed specifically that increasing the ambient temperature from 24˚C to 38˚C decreased the MDT by 4 hours and the TFC by 13 hours (Laefer et al. 2010). In related work, Natanzi et al. (2016) recorded non-linear gains in peak hydration heat and expansive pressure development in higher ambient temperatures in steel pipes for both Dexpan and Bristar (temperature range 2˚C -19˚C).

Such behaviors are directly attributable to the chemical changes in the mixtures. For example, by testing in steel pipes Soeda and Harada (1994) found that increasing ambient

temperature from 5°C to 20°C increased calcium hydroxide ($Ca(OH)_2$) generation in the exothermic reaction of the calcium oxide (CaO) hydration. This work was done with two SCDAs (Table 1): Agent A had almost 20% less free calcium oxide (CaO), while Agent B had almost no alite and a 10% higher belite (dicalcium silicate) content. The mix with almost no alite developed higher expansive pressures, which were credited to the alite delaying the calcium oxide (CaO) hydration. This was confirmed by De Silva et al. (2017) where more alite was identified as reducing the $Ca(OH)_2$) concentration and, in turn, the expansive pressure development. In other research by Soeda et al. (1992), belite was shown to have no impact on expansive pressure development.

Table 1. Chemical composition and main mineral content of expansive demolition agent A and B

	Chemical Composition						
Agent	Igloss	SiO_2	Al_2O_3	Fe_2O_3	CaO	MgO	SO_3
A	1.2	8.5	2.3	1	82.5	0.7	3.5
B	1.2	4.3	1.3	0.5	90.1	0.8	1

Source: Data from Soeda and Harada (1994).

Project Scope and Methodology

To date, there has been no chemical or mineral analysis of post-hydrated SCDAs with respect to ambient temperature. This is important to investigate, as the effect of ambient temperature and local temperature distribution within an SCDA mix is likely to influence local pressure development, as higher temperatures are known to accelerate the exothermic reaction of CaO and calcium hydroxide ($Ca(OH)_2$) formation. Specifically, calcium hydroxide ($Ca(OH)_2$) is known to impact hydration heat development, which in

159 turn influences expansive pressure development. However, work to date has been at
160 temperatures far above those typically encountered in the field (i.e. under 20˚C), where the
161 effect of low and moderate ambient temperature on calcium hydroxide ($Ca(OH)_2$)
162 generation has not been investigated. Additionally, while temperature variation was
163 recently reported (Laefer et al. 2018) to occur within the length of a typical installation
164 (approximately 1 m), the variability and the subsequent performance implications are not
165 well documented. An example of such output is shown in Fig. 1, which was taken with a
166 NEC thermal camera (TH7102WL) on a 50 cm x 5.1 cm pipe filled with Dexpan. Knowing
167 the patterns of such variations can help engineers and contractors more reliably design and
168 possibly optimize field usage.

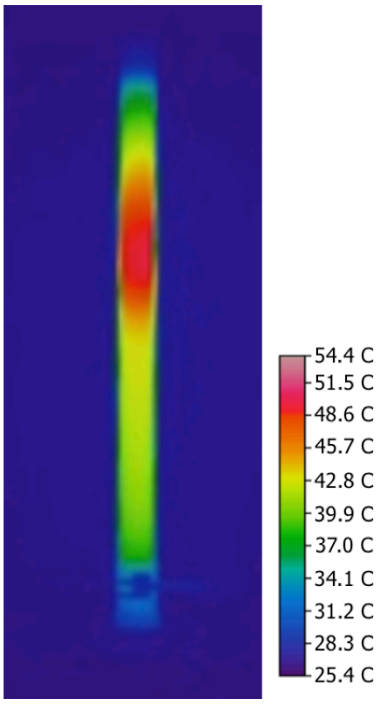

169

170 **Fig. 1.** Thermal image of hydration heat generation through pipe

171

As such, this paper examines the relationship between ambient temperature, calcium oxide (CaO) hydration, and calcium carbonate ($CaCO_3$) generation in 2 commercial SCDAs (Bristar 150 and Dexpan II) tested in the ambient temperature range of 2˚C-19˚C. This work extends the understanding of previous research done at warmer temperatures and improves field usage of SCDAs as it emulates more common ambient field temperatures, which are known to strongly influence maximum pressure development. The percentage of calcium carbonate ($CaCO_3$) generation should be considered in the analysis, as it could reduce the amount of calcium hydroxide ($Ca(OH)_2$) crystals and, subsequently, reduce expansive pressure development. Bristar mainly consists of calcium oxide (CaO) and is designed for temperatures up to 20˚C. Dexpan II, according to its manufacturer is configured for temperatures 10˚C to 25˚C. The chemical compositions of each commercial product are shown in Table 2.

Table 2 Manufacturer provided SCDA ingredients and composition

SCDA Brand	Component	Composition (%by Mass)
Bristar (BASF The Chemical Company n.d.)	Calcium Oxide (CaO)	81-96
	Silicon Dioxide (SiO_2)	1.5-8.5
	Ferric Oxide (Fe_2O_3)	0.2-3.0
	Aluminum Oxide (Al_2O_3)	0.3-5.0
	Magnesium Oxide (MgO)	0-1.6
	Sulfur Trioxide (SO_3)	0.6-4.0
Dexpan (Huynh et al. 2017; KMK Regulatory Services 2016)	Calcium Oxide(CaO)	60-100
	Silicon Dioxide (SiO_2)	5-10
	Diiron Trioxide (Fe_3O_4)	1-5
	Aluminum Oxide (Al_2O_3)	1-5

Each product was tested at 5 different ambient temperatures (2˚C, 5˚C, 10˚C, 17˚C, 19˚C). To investigate material consistency as an outgrowth of the chemical reaction, XRD, TG, and Derivative Thermogravimetric Analysis (DTG) analyses were undertaken for both confined and unconfined samples. DTG and TG tests have been commonly used to characterize calcium oxide (CaO) hydration based on dehydration curves upon heating. The phase composition of the hydrating pastes was studied by XRD.

Experimental Set up

The SCDAs were mixed according to the manufacturers' recommendations (tap water at 15°C and 30% by weight of SCDA). The slurries were poured into seamless, stainless steel pipes with a funnel. The selected 170 mm long pipe (Fig. 2) was deemed adequate to crack a rock or unreinforced concrete specimen to a depth of around 250 mm according to a 70% depth rule developed by Huynh and Laefer (Huynh and Laefer 2009). The pipe was closed only at its lower end, with the upper end open to the air to simulate field conditions. The steel cylinder had a threaded end, which allowed a cap to be screwed securely to its bottom; this facilitated post-test cleaning. A simple clamp was attached to a heavy plate to hold the cylinder upright during testing. To control the ambient temperature, each filled pipe was placed into a temperature-controlled environment.

After each test, the SCDA was observed to be soft (powdery) in the upper, unconfined part of pipe and solid in the lower, confined portion. To investigate this apparent difference, samples from two unconfined and two confined parts of the SCDA samples were collected under five different ambient temperatures and subjected to XRD, TG, and DTG testing. The

mineral composition was investigated by XRD using a Siemens D-5000 diffractometer with Cu Ka1 radiation (λ = 1.5405 Å), operating at voltage 40 kV, and a tube electric current 30 mA. The data were collected across a 2θ range of 10°-70°, with a step size 0.02°, at a scanning speed of 1 sec per step and evaluated using the Siemens "Diffrac Eva" software to identify the mineral phases.

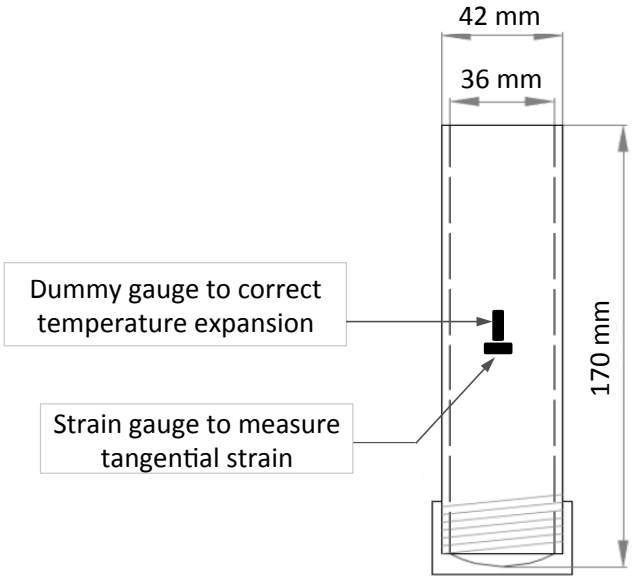

Fig. 2. Steel pipe dimensions

TG in the form of TA Instruments' Thermal Analyst 3000 unit was used for the determination of calcium hydroxide ($Ca(OH)_2$) and calcium carbonate ($CaCO_3$) in hydrated and unhydrated samples. Hydrated SCDA samples were taken from both upper (unconfined) and lower (confined) portions of the pipe and washed with acetone and isopropyl ether. The SCDA was carefully filtered with a vacuum flask and fully dried for 24 hours in a vacuum at a laboratory temperature of 20 (±2°C) to remove the free water and to stop further hydration (Kastis et al. 2006). The dried samples (~50mg) were heated over

the range of 20°C to 1000°C at a constant rate of 10°C /min in an atmosphere of carbon dioxide free nitrogen flowing at 90 cm^3/min.

Experimental Results

X-ray diffraction analyses

The XRD analyses recorded for both unhydrated and hydrated SCDA were also done to investigate the alteration in crystalline phases in both the confined and unconfined parts of hydrated SCDA for both commercial products.

Dry and unhydrated SCDA at ambient temperature

The XRD patterns of dry, unhydrated Bristar and Dexpan showed highly similar chemical compositions (Fig. 3) mostly of calcium oxide (CaO), with the minor addition of cement. The main observed peaks for both products were from the calcium oxide (CaO), as previously reported by the manufacturers (Table 2), with a small amount of calcium hydroxide $Ca(OH)_2$ and calcium carbonate ($CaCO_3$). The presence of calcium hydroxide $Ca(OH)_2$ and calcium carbonate ($CaCO_3$) were due to hydration and carbonation of calcium oxide (CaO), respectively, caused by the CO_2 absorption from the exposure atmosphere. Additionally, other phases investigated in the dry, unhydrated Dexpan were alite [tricalcium silicate (Ca_3SiO_5)], larnite (Ca_2SiO_4), and brownmillerite ($Ca_2(al,Fe)_2O_5$), while the Bristar included mainly calcium hydroxide $Ca(OH)_2$, calcium carbonate ($CaCO_3$) and calcium aluminate cement ($Ca_2Al_2O_5$) (Fig. 3). According to the XRD results in Fig. 3, the peak intensities for calcium oxide (CaO) in Dexpan were significantly higher than those of Bristar

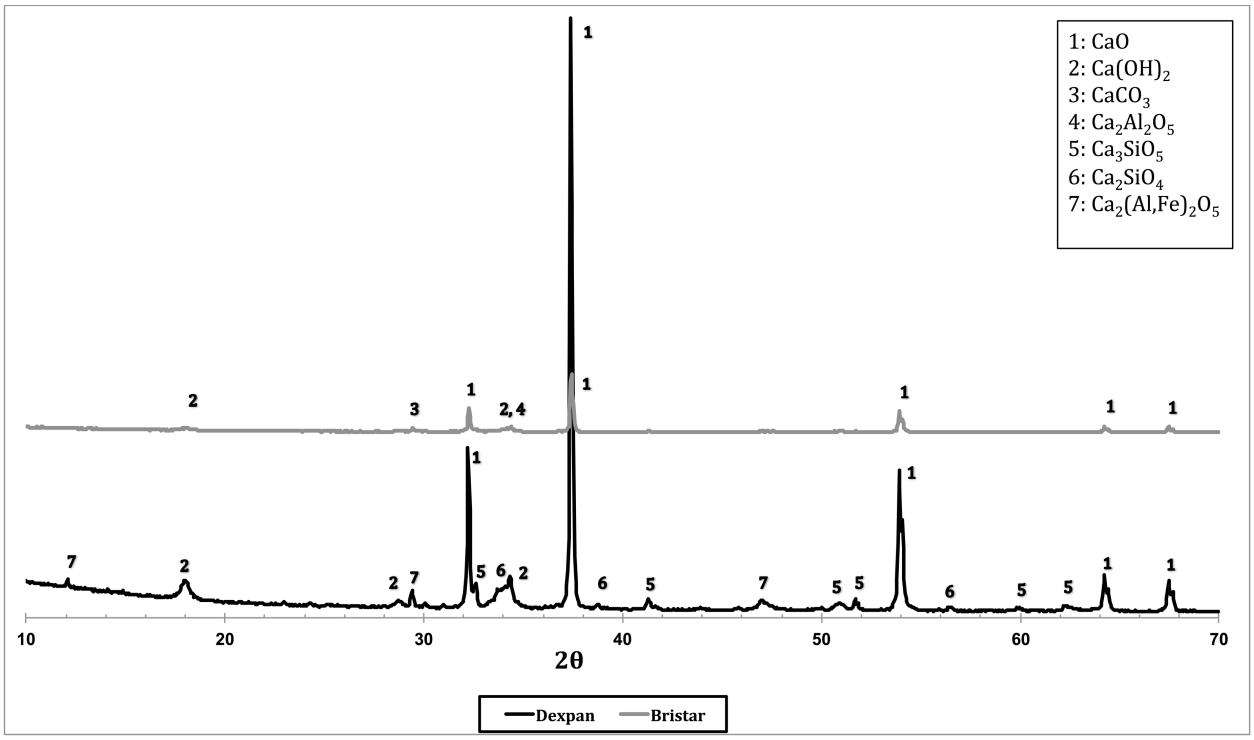

Fig. 3. XRD diffractogram of unhydrated SCDA taken from raw materials

Hydrated SCDA at different ambient temperatures

XRD analyses were also done for the hydrated SCDA to investigate the changes in mineralogy and microstructure after hydration. The physical differences of the upper and lower portions of an SCDA have never before been reported and are important for more optimized product deployment. The chemical phase development in the hydrated upper (soft) and lower (solid) portions of the Dexpan and Bristar can be clearly observed in the XRD diffractograms (Figs. 4-7). Results illustrate significant differences from the unhydrated material (Fig. 3).

Specifically, hydration was less complete in samples from the upper, soft portions of the sample. For the upper, soft portion of the hydrated samples, the XRD patterns of both

brands showed that the hydrated product was mainly calcium hydroxide $Ca(OH)_2$ (Figs. 4-5). In these upper samples, calcium carbonate ($CaCO_3$) was also present due to carbonation of calcium hydroxide $Ca(OH)_2$, which also caused a reduction of calcium hydroxide $Ca(OH)_2$. This peak was clearer in the Dexpan (number 2 in Fig. 4). The XRD diffractogram of the upper Dexpan samples (Fig. 4) also showed the presence of larnite, while Bristar contained alite (Fig. 5). The peak intensity of calcium carbonate ($CaCO_3$) (number 2 in Figs 4-5) in both Dexpan and Bristar showed reductions coincident with the increase in ambient temperature from 2˚C to 19˚C.

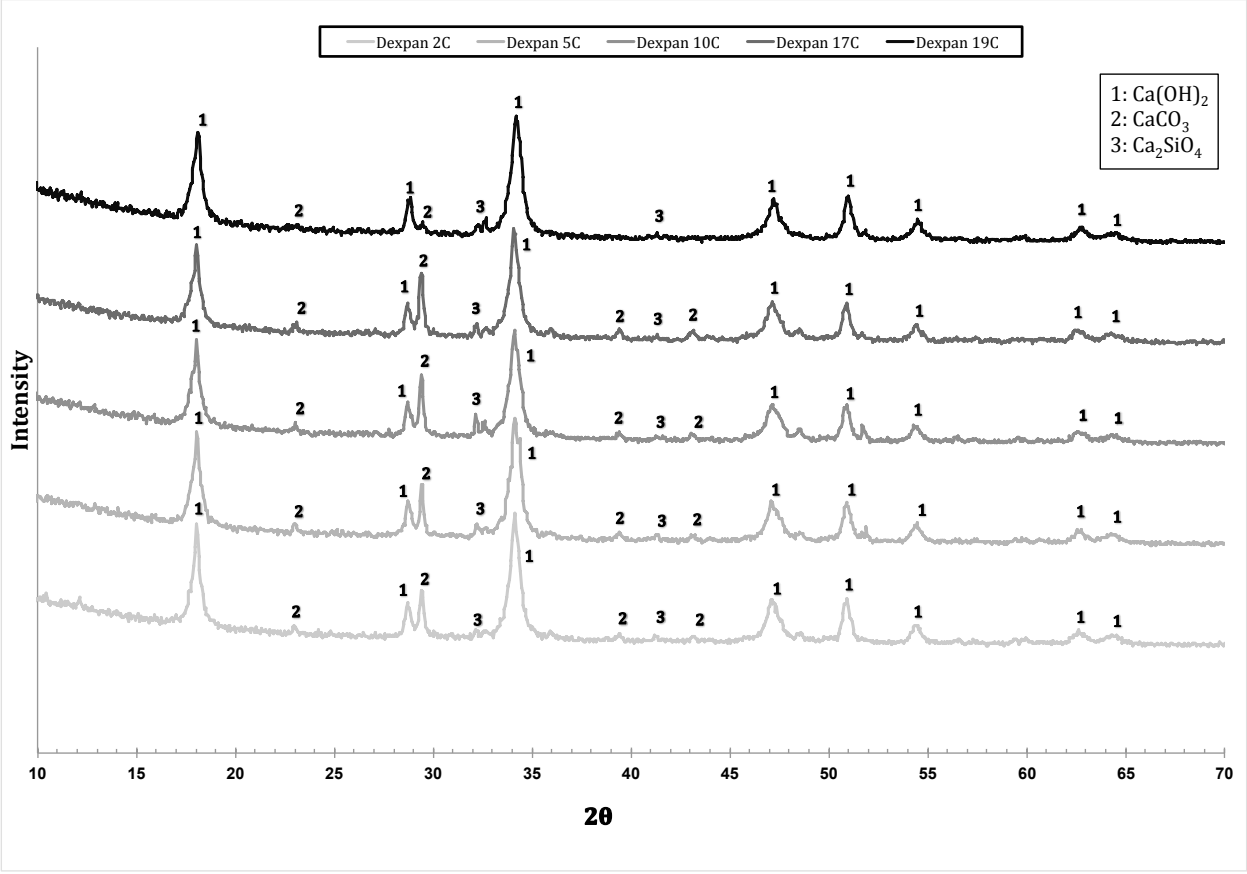

Fig. 4. XRD diffractogram of the upper, soft hydrated part of the Dexpan after exposure to different temperatures

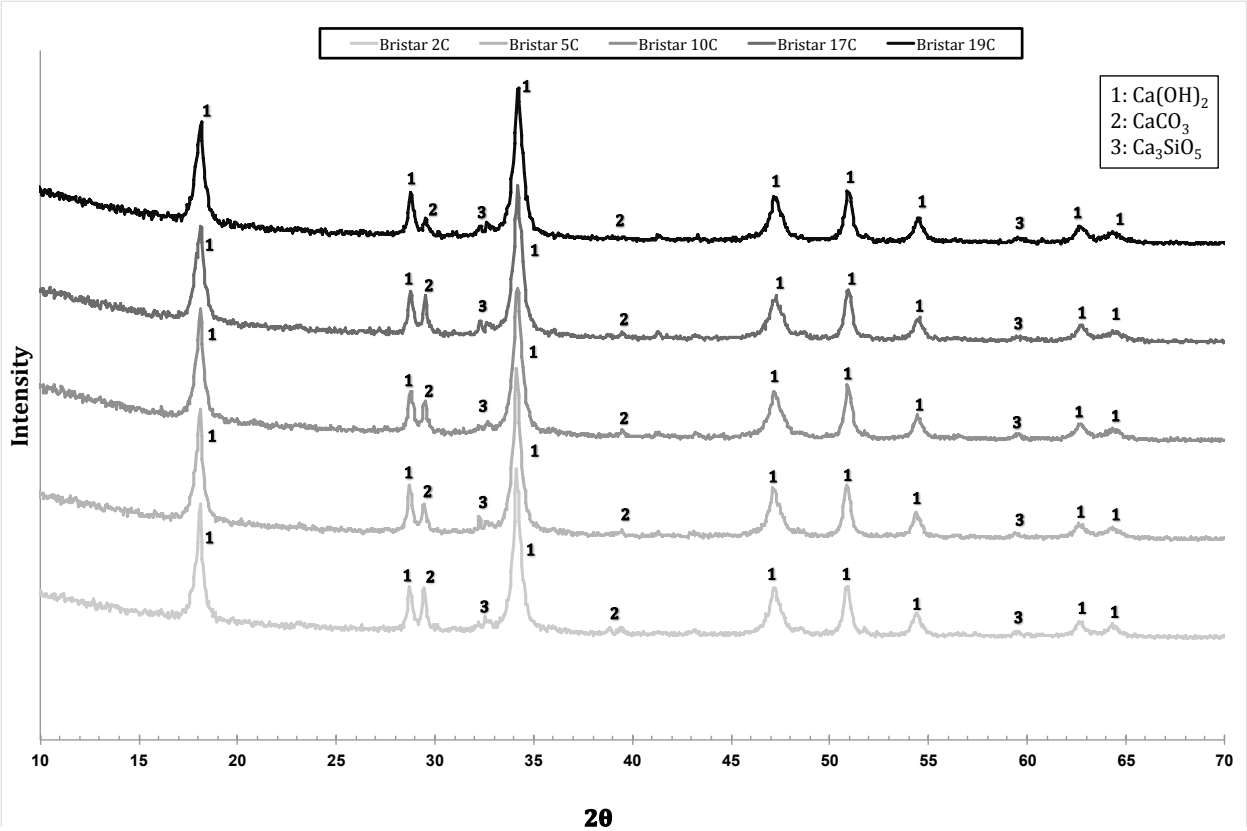

Fig. 5. XRD diffractogram of upper, soft hydrated part of the Bristar after exposure to different temperatures

In the lower (solid) samples of the hydrated SCDA, the overall patterns were similar, with the main peaks of calcium hydroxide $Ca(OH)_2$ (number 1 in Figs. 6-7). A clear peak of larnite (Ca_2SiO_4) was also distinguishable in the XRD pattern in the lower, hydrated Dexpan, which came from the unhydrated Dexpan (as shown in XRD pattern in Fig. 3). The XRD diffractogram showed the presence of alite (Ca_3SiO_5) in the lower, hydrated Bristar. Notably, neither SCDA exhibited a significant calcium carbonate ($CaCO_3$) peak in the lower confined part, where the peak intensity of alite at 2θ of 29.5° in the hydrated Bristar decreased when the ambient temperature increased. Finally, a barium chloride ($BaCl_2$) spot test on dissolved samples identified no sulfate compounds in either brand.

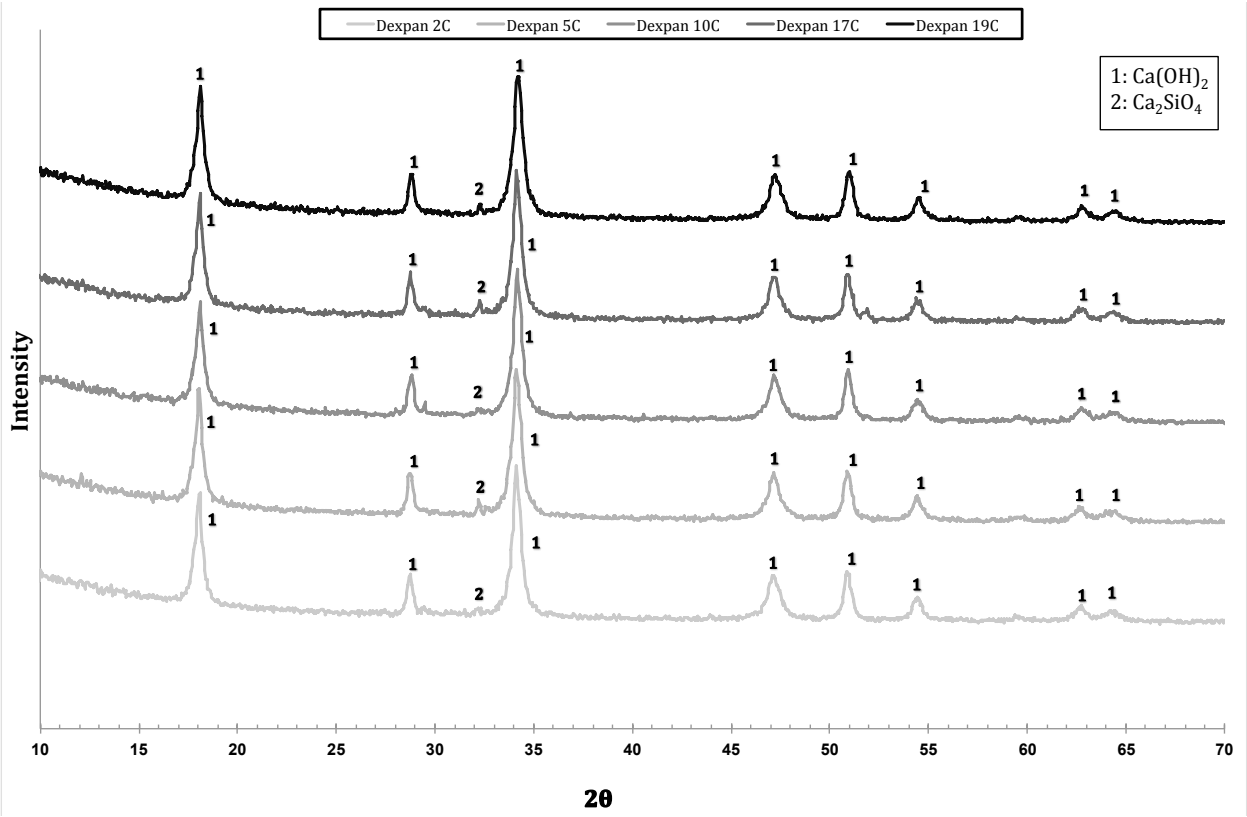

281

282 **Fig. 6.** XRD diffractogram of the lower, solid part of the hydrated Dexpan after exposure to

283 different temperatures

284 **Thermogravimetry and Derivative Thermogravimetric Analysis Results**

285 Thermogravimetry analysis showed unhydrated Dexpan and Bristar containing 17.92%

286 and 23.68% weight of solute/total weight of solution (w/w) $Ca(OH)_2$, respectively. The

287 calcium hydroxide $Ca(OH)_2$ level in the unhydrated Bristar was higher than in the

288 unhydrated Dexpan by almost 6%, which increased the final calcium hydroxide $Ca(OH)_2$

289 level in the hydrated Bristar. Bristar also had 1.70% w/w calcium carbonate ($CaCO_3$), while

290 the Dexpan contained only 1.34 % w/w of the same.

291

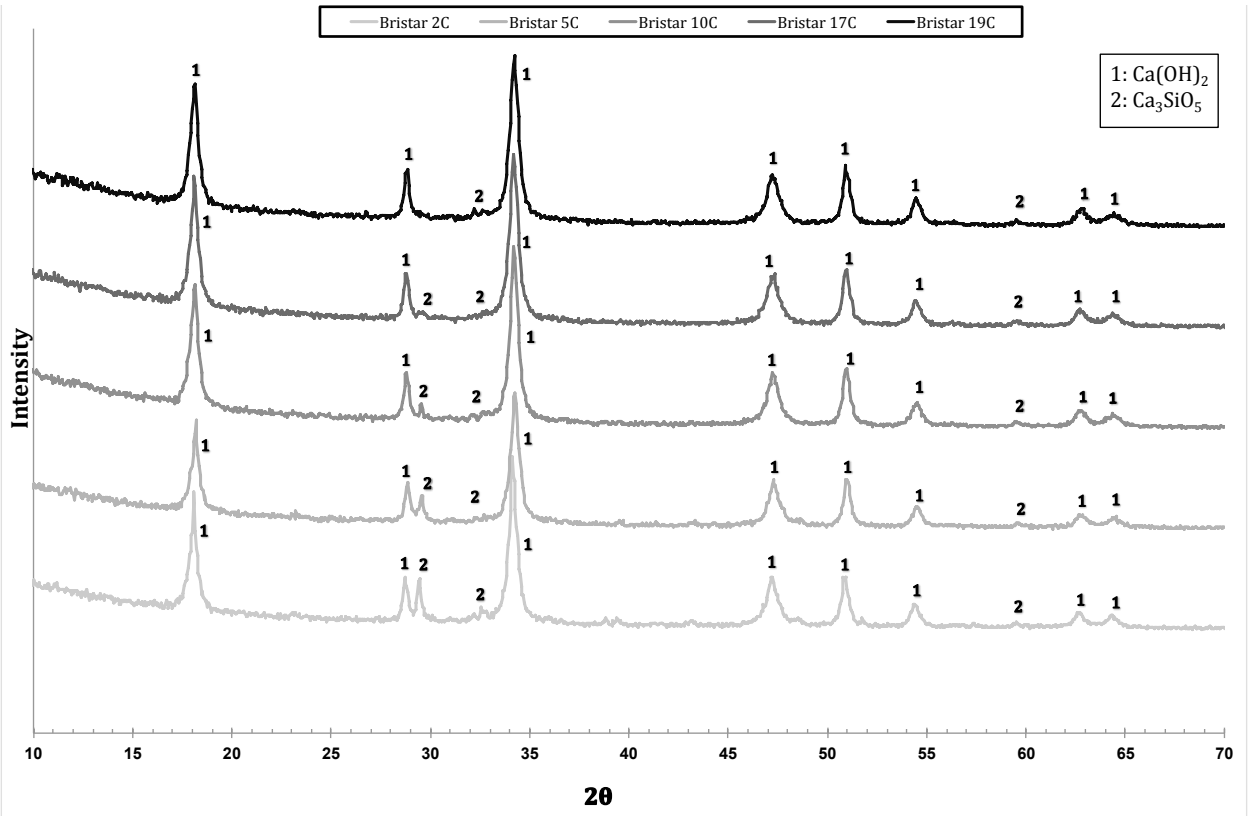

Fig. 7. XRD diffractogram of the lower, solid part of the hydrated Bristar after exposure to different temperatures

Additionally, across the range of temperatures, the calcium hydroxide $Ca(OH)_2$ generation difference between the upper and lower parts in the Dexpan was 6-10%, while it was 9-20% for the Bristar, with calcium hydroxide $Ca(OH)_2$ observed consistently in the lower samples in both products but not in the upper samples (Fig. 8). At the lowest ambient temperature (2˚C), the Bristar's percentage of calcium hydroxide $Ca(OH)_2$ in the lower samples reached 76.87%w/w, while at the same temperature level, the upper sample generated 69.9%w/w calcium hydroxide $Ca(OH)_2$. At the same ambient temperature (2˚C), Dexpan's percentage of calcium hydroxide $Ca(OH)_2$ reached 74.61%w/w for the lower part and 62.43%w/w for the upper. While the difference in the Dexpan was slightly more than

in the Bristar (12.18%w/w vs 6.97%w/w), the phenomenon was clearly the same. Specifically, in all cases, the Dexpan has less calcium hydroxide $Ca(OH)_2$ than the equivalent Bristar samples across the entire temperature range.

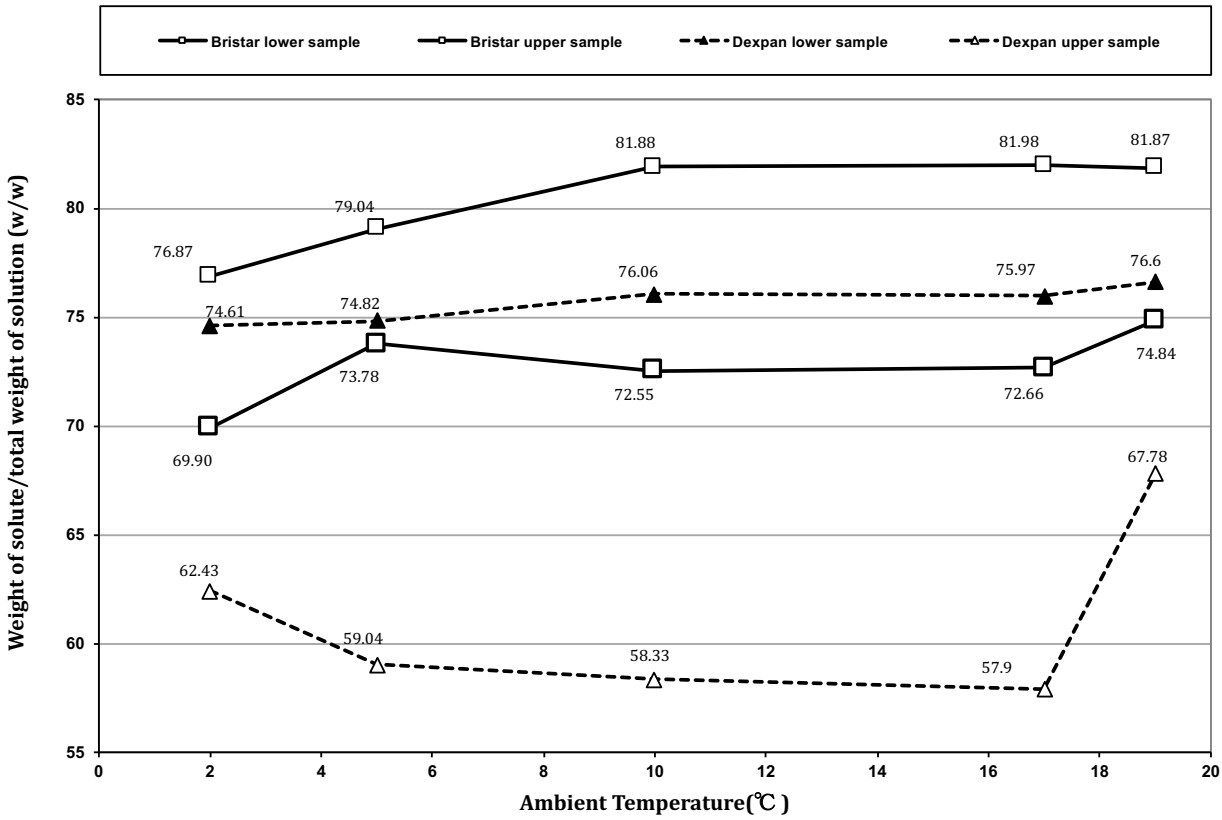

Fig. 8. Calcium hydroxide $Ca(OH)_2$ presentation in TG analysis of the SCDAs

For the lower sample at the lowest ambient temperature (2°C), the Bristar's percentage of calcium hydroxide $Ca(OH)_2$ reached 76.87%w/w, while the Dexpan's level was highly similar at 74.61%w/w. At the highest ambient temperature (19°C), the Bristar level of calcium hydroxide $Ca(OH)_2$ generation reached 81.87%w/w, while the Dexpan's level was 76.60%w/w.

317 In comparison to unhydrated materials, at the highest ambient temperature (19°C), the
318 increases in calcium hydroxide $Ca(OH)_2$ for the lower samples were 345% for Bristar and
319 430% for Dexpan. For both products, the lower samples had almost 10% more calcium
320 hydroxide $Ca(OH)_2$ than in the upper samples.

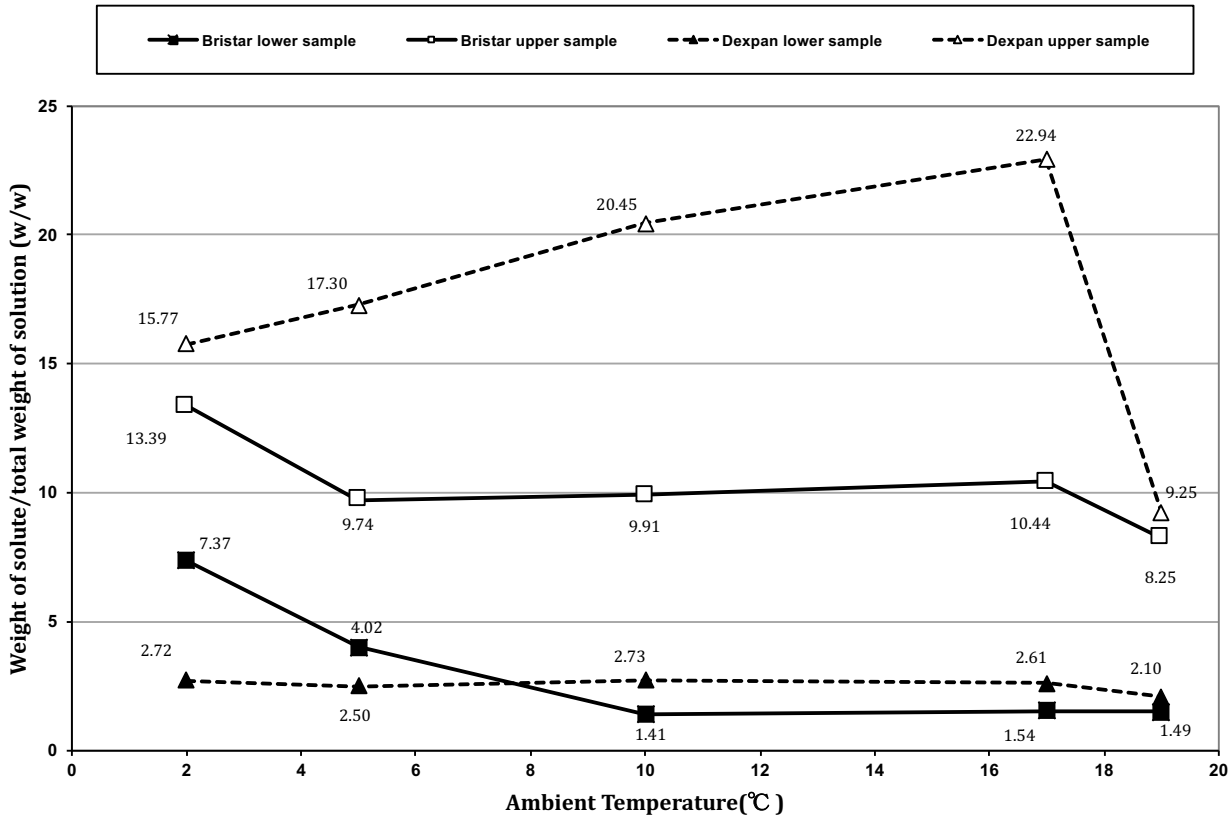

321

322 **Fig. 9.** Calcium carbonate ($CaCO_3$) presentation in TG analysis of the SCDA

323

324 According to the TG analysis, notably higher calcium carbonate ($CaCO_3$) quantities (5-9%
325 w/w for Bristar and 13-20% w/w for Dexpan) appear in the upper, unconfined samples of
326 both products than in their lower confined parts. This is due to the calcium hydroxide
327 $Ca(OH)_2$ carbonation (Fig. 9) and may account for the difference in the physical solidity
328 between the upper and lower portions of the final samples. Upper, unconfined samples are

329 soft, while lower confined samples appear as hard as concrete and must be removed from
330 the pipes at the end of testing with a drill, as they cannot be dislodged by hand.

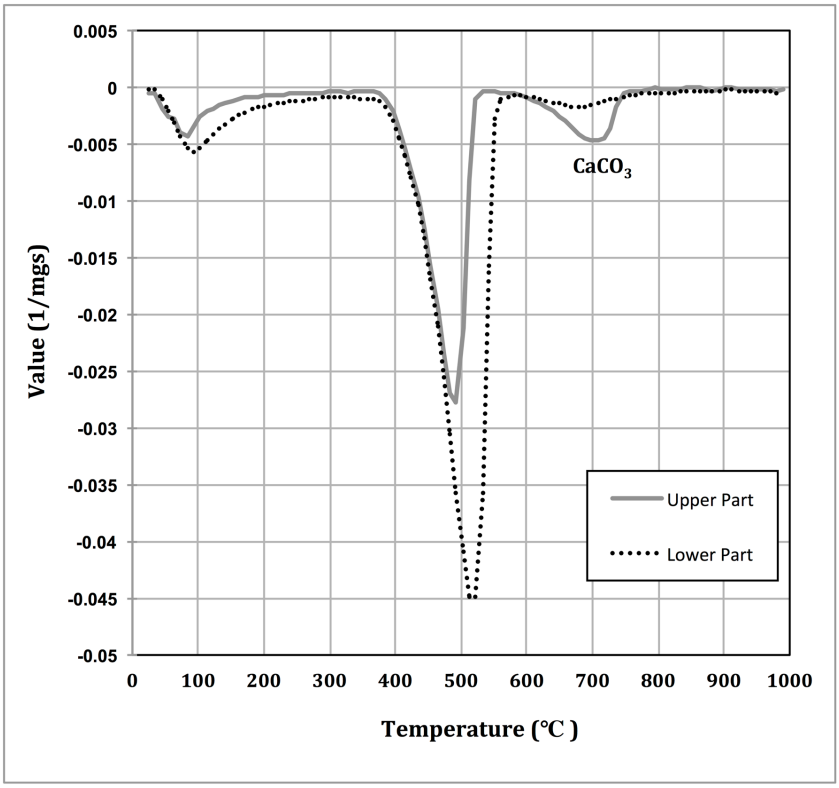

331

332 **Fig. 10.** DTG curves of Dexpan when initially tested at 19˚C

333

334 The DTG curves of Dexpan 19˚C are presented in Fig. 10. The curves can be divided into the
335 three different chemical reactions, which show the three weight loss steps, each
336 corresponding to endothermic processes. From 50˚C to 150˚C there is water removal from
337 the calcium hydroxide $Ca(OH)_2$, which is likely to include most of the calcium silicate
338 hydrates (C-S-H). Several minor steps are likely to have occurred in this phase attributable
339 to capillary pore water, interlayer water, and adsorbed water. The corresponding peaks
340 overlap each other because of the dynamic heating process. Secondly, from 350˚C to 550˚C
341 dehydroxylation of the calcium hydroxide $Ca(OH)_2$ occurs, and the weight loss equals the

water contained in the calcium hydroxide $Ca(OH)_2$. This phase accounts for the main weight loss as can be seen from the relatively sharp curve at this temperature (Fig. 10). Thirdly, from 650°C to 750°C, decomposition of the calcium carbonate ($CaCO_3$) occurs. This was observed in this upper Dexpan sample, thereby indicating the presence of calcium carbonate ($CaCO_3$) (Fig. 10). Similar patterns were obtained for both Dexpan and Bristar across the ambient temperature range.

Discussion

Arguably, there are three important findings in the work reported herein. The first relates to XRD patterns, the second involves the distribution of calcium hydroxide after usage, and the third concerns the thermal behavior within the sample.

XRD patterns

The main XRD peaks were identified herein as calcium oxide (CaO), as previously identified by Tang et al. (2017) for dry unhydrated SCDA. Similar XRD patterns to those reported herein (Figs. 4 and 5) were previously shown by Shahraki et al. (2011) for hydrated SCDA when they mixed the expansive agent Katrock with water (Fig. 11). That research and the experiments undertaken herein show that the main peaks in XRD plots belong to the primary hydration product, calcium hydroxide $Ca(OH)_2$. The XRD pattern reported by Shahraki et al. (2011) is more similar to the Bristar XRD pattern than that of the Dexpan reported herein. The XRD results shown herein demonstrate that the hydration of calcium oxide CaO is the main chemical reaction that happens and generates the SCDA expansive pressure development and volumetric expansion. These results are in agreement with experimental results by De Silva et al. (2017, 2018) including XRD analyses for hydrated

364 Bristar 100 after 4 h of hydration. Experimental results herein also show the presence of
365 larnite in the upper and lower Dexpan samples, while alite was the main phase in the
366 equivalent Bristar samples at all ambient temperatures. De Silva et al. (2017) also detected
367 alite in hydrated Bristar and observed that the combination of both free lime and alite
368 dissolution adds calcium hydroxide $Ca(OH)_2$ to the system. This was confirmed across the
369 full temperature range by the TG results herein showing greater calcium hydroxide
370 $Ca(OH)_2$ concentration in Bristar rather than in Dexpan. Notably, previous work Natanzi et
371 al. (2016) showed that Bristar generated more expansive pressure than Dexpan under the
372 same ambient temperature.

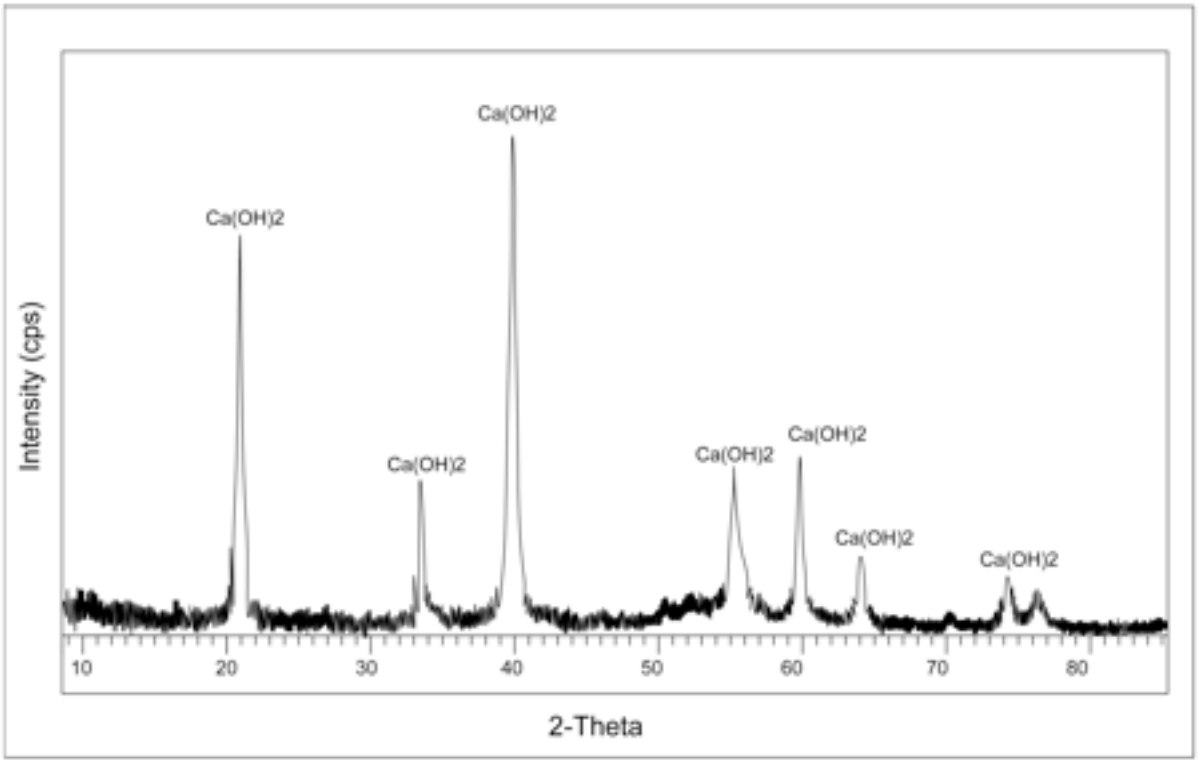

373

374 **Fig. 11.** XRD pattern of hydrated SCDA (Shahraki et al. 2011)

375

Calcium hydroxide distribution

In the research undertaken herein, the TG analysis also showed that higher ambient temperatures resulted in greater percentages of calcium hydroxide, $Ca(OH)_2$. In contradiction to these results, Harada et al. (1993) initially reported that CaO hydration is independent of temperature—based on tests on an expansive demolition agent (water to SCDA ratio 25%) in a 42.7 cm diameter x 15 cm high steel pipe at ambient temperatures of 20˚C and 30˚C. The degree of hydration of CaO was calculated as the percentage of full hydration (100%) when a specimen was placed in water at 30˚C for 66 hours and then cured for three days in steam at 65˚C. Shortly thereafter, Soeda and Harada reported a reversal of this position (Soeda and Harada 1994) where temperature was observed to have a direct influence on calcium hydroxide $Ca(OH)_2$ generation. Further work from that group confirmed this latter finding (Soeda et al. 1994), where faster SCDA hydration velocities were recorded in higher temperatures.

The TG results reported herein extend this understanding into the lower temperature ranges within which the level of hydration of calcium oxide (CaO) into calcium hydroxide ($Ca(OH)_2$) was higher as the temperature increased. The TG analyses reported herein also showed a higher percentage of calcium hydroxide, $Ca(OH)_2$, in the hydrated Bristar over that of the Dexpan in the upper and lower both parts. These results of the effects of calcium hydroxide, $Ca(OH)_2$, parallel the previously reported higher expansive pressures in the Bristar over the Dexpan in these pipe-based samples across this cold to cool ambient temperature range (Natanzi et al. 2016). It is important to consider that in the lower confined part, hydration is more complete than in the upper unconfined part and this could

399 directly influence the expansive pressure development. Laefer et al.'s (2018) experimental
400 work also showed that expansive pressure development was higher in the lower confined
401 part of 700 mm pipe than the upper unconfined part.
402
403 Early experimental work by Soeda et al. (1994) showed that greater hydration levels
404 resulted in higher expansive pressure development. At 24 hours, they measured expansive
405 pressures of 35 MPa at 5˚C and 42 MPa at 20˚C for a fast acting SCDA in the middle of a 1 m
406 high x 38 mm diameter specimen tested in a steel pipe. Experimental results by Natanzi et
407 al. (2016) in the range of 2˚C to 19˚C also definitively showed that higher ambient
408 temperatures result in greater hydration heat levels, which translate to higher expansive
409 pressure development.

410 **Thermal behavior**

411 Thermal behavior of SCDAs was considered herein with respect to TG and DTG test results
412 from the ambient temperature to 1000˚C. In earlier work research by Shahraki et al. (2011)
413 differential thermal analysis on three types of CaO-based expansive agents showed the
414 same pattern as the research herein (Fig. 12). Notably, however, they observed an
415 endothermic peak at 800-900˚C versus the endothermic peak observed at 350-550˚C in the
416 research herein. The difference is probably attributable to various chemical components in
417 the various SCDAs. In the analysis by Nocun-Wczelik et al. (2012), three peaks were
418 observed in expansive cements and expansive additives. The first peak was at almost
419 350˚C, the second at 480˚C, and the third at 650- 750˚C. The second peak in their research,
420 which corresponds to the dehydration of calcium hydroxide $Ca(OH)_2$ is almost in the same

range as that reported herein, while the third peak happened in exactly the same range (650-750˚C). In research by El-Didamony and Haggag (1978) on a 15 minute old expansive cement, the first endotherm occurred in the range of 180-280˚C, and the other two peaks were between 450-550˚C and 800-900˚C (Fig. 13).

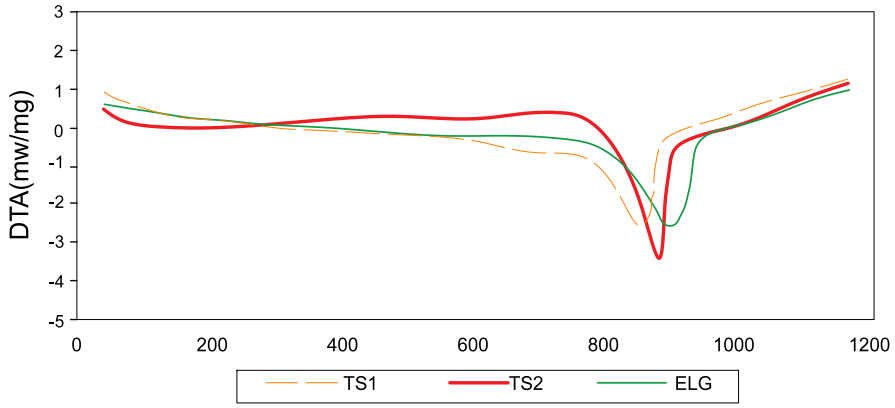

Fig. 12. Differential thermal analysis on CaO based expansive agents (Shahraki et al 2011)

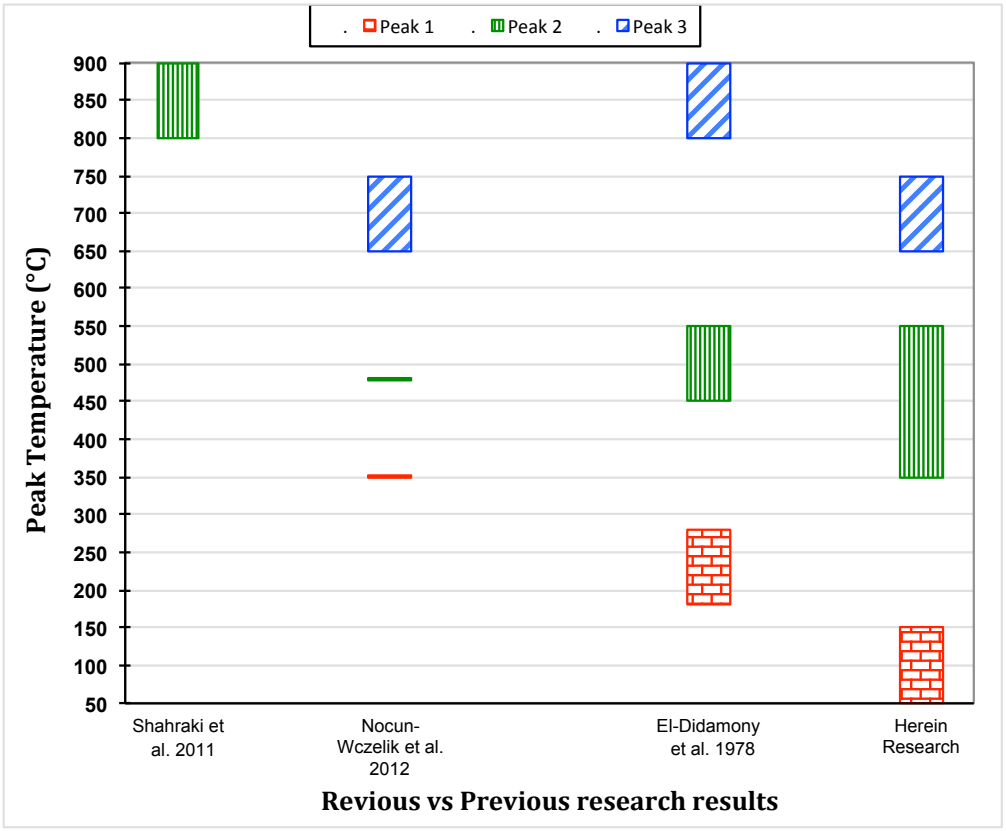

Fig. 13. Comparison of DTG peaks

Conclusions

In this paper, a series of chemical analyses explored the effect of cool and moderate temperatures (2˚C -19˚C) on two Soundless Chemical Demoliton Agents (SCDAs) (Dexpan and Bristar) in sections of steel pipe. The SCDAs had been observed to be soft (powdery) in the upper, unconfined part of the pipes while the lower confined part SCDA was solid. To investigate this apparent difference, the mineral composition of each sample was investigated by X-ray diffraction (XRD). Thermogravimetry (TG) and Derivative Thermogravimetric Analysis (DTG) methods were also used for characterizing the hydration products based on their dehydration curves on heating. XRD results for unhydrated Dexpan and Bristar showed that they mostly contained calcium oxide CaO with minor additions of cement. The Dexpan also contained tricalcium silicate (Ca_3SiO_5)[alite], larnite, and brownmillerite, while the Bristar had calcium aluminate cement. Results showed that the main hydration products in the soft upper and solid lower parts of the pipe were calcium hydroxide $Ca(OH)_2$. Hydration was more complete in the lower, solid portions of the samples. XRD results showed the presence of $CaCO_3$ due to carbonation of $Ca(OH)_2$ in the upper part of the pipes.

TG/DTG results showed that the calcium hydroxide $Ca(OH)_2$ level in the unhydrated Bristar was higher than that in the unhydrated Dexpan by almost 6%, which increased the final calcium hydroxide $Ca(OH)_2$ level in the hydrated Bristar. TG results also showed that calcium hydroxide $Ca(OH)_2$ levels were higher in the lower part of the materials than in the upper part by almost 10% for both products. Calcium carbonate ($CaCO_3$) was higher in the upper part, and its formation was due to the carbonation of $Ca(OH)_2$ and being exposed to

the air. Also, the results indicated that increasing ambient temperature can increase calcium hydroxide $Ca(OH)_2$ and decrease calcium carbonate ($CaCO_3$) even at cold and cool temperatures. At as little as 2˚C, the process occurs, with higher calcium hydroxide $Ca(OH)_2$ generation impacting the heat of hydration development, which in turn influences expansive pressure development directly.

Acknowledgments

The authors would like to thank Mr Derek Holmes, lab technician, University College Dublin for his tireless efforts in the lab throughout the research, Mr C. Aspiotis for his contribution in XRD and TG experiments. This work was supported by Science Foundation Ireland [12/ERC/12534].

Data Availability Statement

The raw and processed data required to reproduce these findings cannot be shared at this time due to technical or time limitations.

References

Aqel, M. A., and Panesar, D. K. (2017). "Delayed Ettringite Formation in Concrete Containing Limestone Filler." *ACI Special Publication*, 320, 43.1-43.12.

BASF The Chemical Company. (n.d.). *Bristar Material Safety Data Sheet*.

Cohen, M. D. (1983). "Theories of expansion in sulfoaluminate - type expansive cements: Schools of thought." *Cement and Concrete Research*, 13(6), 809–818.

Cohen, M. D., and Richards, C. W. (1982). "Effects of the particle sizes of expansive clinker on strength-expansion characteristics of type K expansive cements." *Cement and Concrete Research*, 12(6), 717–725.

De Silva, V. R. S., Ranjith, P. G., Perera, M. S. A., Wu, B., and Rathnaweera, T. D. (2017). "Investigation of the mechanical, microstructural and mineralogical morphology of soundless cracking demolition agents during the hydration process." *Materials Characterization*, 130(May), 9–24.

De Silva, V. R. S., Ranjith, P. G., Perera, M. S. A., Wu, B., & Rathnaweera, T. D. (2018). A modified, hydrophobic soundless cracking demolition agent for non-explosive demolition and fracturing applications. *Process Safety and Environmental Protection,* 119, 1-13.

Dowding, C. H., and Labuz, J. F. (1982). "Fracturing of rock with expansive cement." *Journal of Geotechnical Engineering ASCE*, 109, 1288–1299.

El-Didamony, H., and Haggag, M. Y. (1978). "Studies on expansive cement II. Hydration kinetics, surface properties and microstructure." *Cement and Concrete Research*, 7, 351–358.

Étkin, M. B., and Azarkovich, A. E. (2006). "Effect of non-explosive splitting compounds and

rational work parameters." *Power Technology and Engineering*, 40(5), 287–292.

Goto, K., Kojima, K., and Watabe, K. (1988). "The mechanism of expansive pressure and blow-out of static demolition agent." *Second International RILEM Symposium on demolition and reuse of concrete and masonry*.

Harada, T., Soeda, K., Idemistzu, T., and Watanabe, A. (1993). "Characteristics of expansive pressure of an expansive demolition agent and the development of new pressure transducers." *Proceedings of the Japan Society of Civil Engineers*, 478, 95–109.

Hayashi, H., Soeda, K., Hida, T., and Kanbayashi, M. (1993). "Non-explosive demolition agent in Japan." *Demolition and Reuse of Concrete and Masonry: Proceedings of the Third International RILEM Symposium*, E. K. Lauritzen, ed., CRC Press, 231–241.

Hinze, J., and Brown, J. (1994). "Properties of Soundless Chemical Demolition Agents." *Journal of Construction Engineering and Management*, 120(4), 816–827.

Huynh, M. P., and Laefer, D. F. (2009). "Expansive cement and soundless chemical demolition agents: state of technology review." *11th Conference on Science and Technology*, Ho Chi Minh City, Vietnam, 95–104.

Huynh, M. P., Laefer, D. F., McGuill, J., and White, A. (2017). "Temperature-related performance factors for chemical demolition agents." *International Journal of Masonry Research and Innovation*, 2(2–3), 220–240.

Kastis, D., Kakali, G., Tsivilis, S., and Stamatakis, M. G. (2006). "Properties and hydration of blended cements with calcareous diatomite." *Cement and Concrete Research*, 36(10), 1821–1826.

KMK Regulatory Services. (2016). *Safety data sheet: DEXPAN (Non-Explosive Demolition Agent)*.

514 Laefer, D. F., Ambrozevitch-Cooper, N., Huynh, M. P., Midgette, J., Ceribasi, S., and Wortman,
515 J. (2010). "Expansive fracture agent behaviour for concrete cracking." *Magazine of*
516 *Concrete Research*, 62(6), 443–452.
517 Laefer, D.F., Natanzi, A. S., Zolanvari, S.M.I . (2018). "Impact of thermal transfer on
518 hydration heat of a Soundless Chemical Demolition Agents. " *Construction and Building*
519 *Materials*, Elsevier, 187, 348–359.
520 https://doi.org/10.1016/j.conbuildmat.2018.07.168.
521 Mather, B. (1970). *Expansive Cements*. Vicksburg, MS.
522 Mehta, P. K. (1973). "Mechanism of expansion associated with ettringite formation." *Cement*
523 *and Concrete Research*, 3(1), 1–6.
524 Natanzi, A. S., Laefer, D. F., and Connolly, L. (2016). "Cold and moderate ambient
525 temperatures effects on expansive pressure development in soundless chemical
526 demolition agents." *Construction and Building Materials*, Elsevier Ltd, 110, 117–127.
527 Natanzi, A.S. and Laefer, D.F. (2014). "Using chemicals as demolition agents near historic
528 structures." In 9th International Conference on Structural Analysis of Historical
529 Constructions, Mexico City, Mexico, 14-17 October, 2014.
530 Nocuń-Wczelik, W., Bochenek, A., and Migdâ, M. (2012). "Calorimetry and other methods in
531 the studies of expansive cement hydrating mixtures." *Journal of Thermal Analysis and*
532 *Calorimetry*, 109(2), 529–535.
533 Onoda Cement Company. (1980). *Bristar—Nonexplosive Demolition Agent*. Tokyo, Japan.
534 Polivka, M. (1973). "Factors Influencing Expansion of Expansive Cement Concretes." *ACI*
535 *Special Publication*, 38, 239–250.
536 Shahraki, B. K., Mehrabi, B., Gholizadeh, K., and Mohammadinasab, M. (2011). "Thermal

behavior of calcite as an expansive agent." *Journal of Mining and Metallurgy, Section B: Metallurgy*, 47(1), 89–97.

Soeda, K., and Harada, T. (1994). "The Mechanics of Expansive Pressure Generation." *Concrete Library of JSCE*, (23), 121–135.

Soeda, K., Hida, T., Hayashi, H., and Kanbayashi, M. (1992). "The Influence of Additives on the Expansive Stress of Quick Lime." *Gypsum & Lime*, 237, 9–14.

Soeda, K., Tsuchiya, K., Matsuhisa, M., and Harada, T. (1994). "The properties of the expansive stress of non-explosive demolition agent in long period of time." *Gypsum & Lime*, 248, 37–43.

Tang, Y., Yuan, L., Xue, J., & Duan, C. (2017). Experimental study on fracturing coal seams using CaO demolition materials to improve permeability. *Journal of Sustainable Mining*, *16*(2), 47-54.

Taylor, H. F. W., Famy, C., and Scrivener, K. L. (2001). "Delayed ettringite formation." *Cement and Concrete Research*, 31(5), 683–693.